

Control of thermal and photochemical reaction pathways by $-\text{NO}_2$ pendants in macrocyclic complexes

The redox photochemistry of $\text{Cu}(10\text{-methyl-1,4,8,12\text{-tetraazacyclopentadecan-10-Y})^{2+}$, $\text{Y} = \text{NO}_2, \text{NH}_2$, in charge transfer and ligand field excited states

B. Ellis, G. Smith, G. Ferraudi*

Radiation Laboratory, University of Notre Dame, Notre Dame, IN 46556, USA

Received 3 February 2004; received in revised form 3 May 2004; accepted 14 May 2004

Available online 31 July 2004

Abstract

The irradiation of $\text{Cu}(10\text{-methyl-1,4,8,12\text{-tetraazacyclopentadecan-10-NO}_2)\text{X}^+$, $\text{X} = \text{halide}, \text{HCO}_2^-, \text{CH}_3\text{CO}_2^-, \text{and } \text{C}_6\text{H}_5\text{CH}_2\text{CO}_2^-$, in deaerated CH_3CN or CH_3OH at 350 nm resulted in the reduction of the pendent $-\text{NO}_2$ to $-\text{NO}$. Flash photolysis revealed the formation of the nitroso products via the photo-induced oxidation of the axial ligand X^- . Intermediates in a 10 ns–1 s time scale have been tentatively assigned as species formed by the addition of the X^\bullet radicals to the $-\text{NO}_2$. Similar redox processes were observed when the irradiation of the complexes was carried out in the ligand field band, $\lambda_{\text{exc}} = 560$ nm. Conversion of the ligand field excited states to X^- to $\text{Cu}(\text{II})$ charge transfer excited state account for the photoreactivity of the former excited states.

© 2004 Elsevier B.V. All rights reserved.

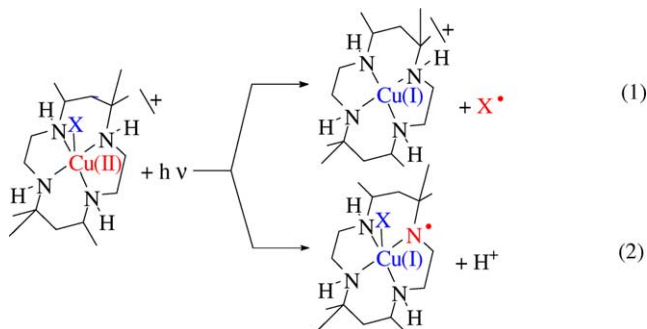
Keywords: Thermal and photochemical reaction pathways; $-\text{NO}_2$ pendants; Macrocyclic complexes

1. Introduction

The interest in transition metal complexes of macrocyclic ligands with pendent groups has been stimulated because of their novel properties and the diverse applications as photo-molecular devices, sensors, and light energy storage [1–17]. Macrocyclic complexes of $\text{Zn}(\text{II})$ with pendent amino groups have been proposed as model compounds of $\text{Zn}(\text{II})$ containing enzymes [1,4,12,16,17]. In these model compounds, the enzymatic activity has been related to the ability of the pendent amino group to bind/unbind to and from the metal center as a function of medium conditions. In other examples, interactions between the pendent group and the metal ion affect the photochemical properties of the macrocyclic complex and/or those of the pendent group. Several molecular systems, where a fluorescent chromophore is linked to a cyclic or open quadridentate ligand, have been communicated in literature reports [18–23]. Complexation with a transition metal ions quenches the chromophore's fluores-

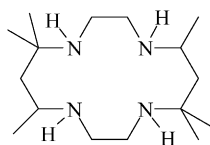
cence and the ligands can be sensitive sensors of metal ions or molecular switches of the fluorescence.

In the photochemistry of $\text{Cu}(5,7,7,12,14,14\text{-hexamethyl-1,4,8,11\text{-tetraazacyclotetradecane})$ (halide) $^+$, **Scheme 1**, the photo-oxidation of axially co-ordinated X^- competes with the oxidation of the macrocycle, Eqs. (1) and (2) [24].

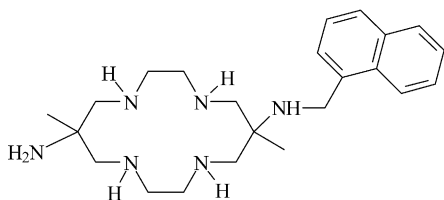


By contrast to these complexes, $\text{Cu}(\text{trans-6-(1-naphthylmethylamino)-6,13-dimethyl-1,4,8,11\text{-tetraazacyclotetradecan-13-amine}})^{2+}$, **Scheme 1**, undergoes no chemical transformations when it is irradiated in the UV and the luminescence of the pendent naphthyl is quenched [25]. In

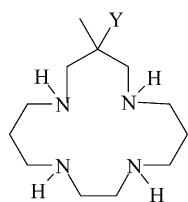
* Corresponding author. Fax: +1 574 631 8068.
E-mail address: ferraudi.1@nd.edu (G. Ferraudi).



5,7,7,12,14,14-hexamethyl-1,4,8,11-tetraazacyclotetradecane



trans-6-(1-naphthalenylmethylamino)-6,13-dimethyl-1,4,8,11-tetraazacyclotetradecan-13-amine

10-methyl-1,4,8,12-tetraazacyclotetradecan-10-Y
and Y = NO₂ or NH₂

Scheme 1.

In addition to the metal ion-pendent group interactions that deactivate electronic excited states, the pendants in the macrocycle must be able to function as scavengers of the primary photoproducts and change the reaction pathway. The effects of pendent –NH₂ and –NO₂ groups in the photochemistry of saturated tetraazamacrocyclic complexes of Cu(II) was investigated in this work.

2. Experimental

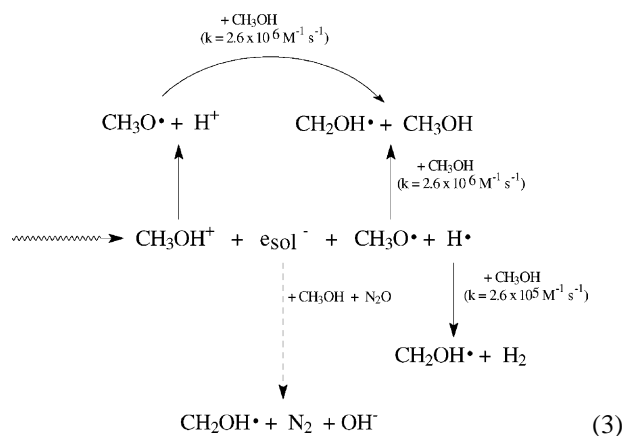
2.1. Photochemical procedures

Optical density changes occurring in a time scale longer than 10 ns, were investigated with a flash photolysis apparatus described elsewhere. In these experiments, 20 ns flashes of 351 nm light were generated with a Lambda Physik SLL-200 excimer laser [26,27]. The concentrations of the complexes in solutions used for these experiments were adjusted by means of the UV–vis spectrum. Their concentrations insured the homogeneous photogeneration of intermediates within the volume of irradiated solution, i.e., optical densities equal to or less than 0.1 in a 1 cm optical path at 351 nm. The liquids were deaerated with streams of ultrahigh-purity N₂ before and during the irradiations. A flow–stop system brought fresh solution to the reaction cell before each irradiation when the decomposition of the complexes and/or formation of products interfered with the optical measurements.

Steady-state irradiations were carried out with light from a 350 nm Rayonet lamp. Light intensities, $5 \times 10^{-4} \geq I_0 \geq 1 \times 10^{-4}$ Einstein dm⁻³ min⁻¹, were measured with Parker's actinometer [8]. Photolytes were irradiated in a 200 cc gas tight cell for the determination of products. The volume of the photolyzed solutions was reduced to 10 cc by evaporation under vacuum at RT. The reaction products and solvent were separated from the Cu complexes and other salts, e.g., NaOCOCH₂C₆H₅, by a high vacuum, $\sim 10^{-5}$ Torr, trap to trap distillation/sublimation. Organic solvents, CH₃CN or CH₃OH, distilled at room temperature while photolysis products, e.g., C₆H₅CH₂OH and C₆H₅CH₂CH₂C₆H₅CH₂, were distilled between room temperature and 95 °C. The distillates were analyzed by GC–MS.

2.2. Pulse radiolysis

Pulse radiolysis experiments were carried out with a model TB-8/16-1S electron linear accelerator. The instrument and computerized data collection for time-resolved UV–vis spectroscopy and reaction kinetics have been described elsewhere in the literature [28–30]. Thiocyanate dosimetry was carried out at the beginning of each experimental session. The details of the dosimetry have been reported elsewhere [28–30]. The procedure is based on the concentration of (SCN)₂•⁻ radicals generated by the electron pulse in a N₂O-saturated 10⁻² M SCN⁻ solution. In the procedure, the calculations were made with G = 6.13 and an extinction coefficient, $\epsilon = 7.58 \times 10^3$ M⁻¹ cm⁻¹ at 472 nm, for the (SCN)₂•⁻ radicals [28–30]. In general, the experiments were carried out with doses that in N₂-saturated aqueous solutions resulted in $(2.0 \pm 0.1) \times 10^{-6}$ M to $(6 \pm 0.3) \times 10^{-6}$ M concentrations of e_{aq}⁻. In these experiments, solutions were deaerated with streams of the O₂-free gasses N₂ or N₂O. In order to irradiate a fresh sample with each pulse, an appropriate flow of the solution through the reaction cell was maintained during the experiment. Radiolyses with ionizing radiation of CH₃OH and CH₃OH/H₂O mixtures have been reported elsewhere in the literature [31–33]. These studies have shown that pulse radiolysis can be used as a convenient source of e_{sol}⁻ and CH₂OH• radicals. The sequence of events in the radiolysis of these solvents is shown in Eq. (3).



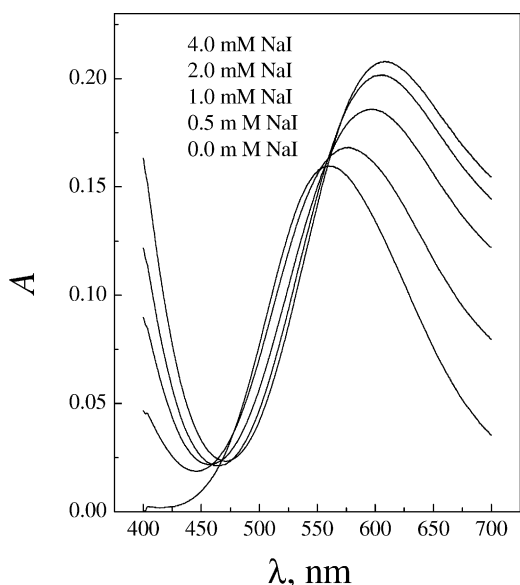


Fig. 1. Dependence of the LF absorption band of $\text{Cu(L-NO}_2\text{)}^{2+}$ on the concentration of I^- . Spectra recorded with methanolic solutions 1.5×10^{-3} M $\text{Cu(L-NO}_2\text{)}^{2+}$ and given concentrations of NaClO_4 to produce a 10^{-2} M ionic strength.

Since, e_{sol}^- and $\bullet\text{CH}_2\text{OH}$ have large reduction potentials, i.e., -2.8 V versus NHE for e_{sol}^- and -0.92 V versus NHE for $\bullet\text{CH}_2\text{OH}$, they have been used for the reduction of coordination complexes and for the study of electron transfer reactions. The yield of e_{sol}^- in CH_3OH ($G \approx 1.1$) is about a third of the G -value in the radiolysis of H_2O ($G \approx 2.8$) [31]. In solutions where e_{sol}^- was scavenged with N_2O , [33], the $\text{CH}_2\text{OH}\bullet$ radical appears to be the predominant product (yield > 90%) of the reaction between CH_3OH and $\text{O}\bullet^-$.

2.2.1. Materials

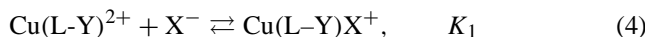
Published procedures were used for the preparation of $[\text{Cu(L-Y)}](\text{ClO}_4)_2$ complexes, where $\text{L} = 10\text{-methyl-1,4,8,12-tetraazacyclopentadecan-10-}$ and $\text{Y} = \text{NO}_2$ or NH_2 , Scheme 1 [34–36]. The materials from these preparations were recrystallized three times from their aqueous solutions by the addition of solid NaClO_4 and the purity was assessed by means of the UV–vis spectrum. The extinction coefficients of these compounds and those communicated in the literature differed by less than 0.2% [34–36].

3. Results

3.1. Species in solution

The coordination of various anions, $\text{X}^- = \text{halide, HCO}_2^-, \text{CH}_3\text{CO}_2^-$, to $\text{Cu(L-NO}_2\text{)}^{2+}$ in non-aqueous solvents was followed by means of the changes in the UV–vis spectrum of the complex, Fig. 1. Displacements of the ligand field, LF, absorption band with halide concentration, $[\text{X}^-] \leq 4 \times 10^{-2}$ M, were those expected for the formation

of Cu(L-Y)X^+ ($\text{Y} = \text{NO}_2$ or NH_2), Eq. (4).



Solvent dependent association constants, Eq. (5), were calculated for carboxylates, halides and pseudohalides by means of the spectral changes in the region of the ligand field bands.

$$K_1 = \frac{[\text{Cu(L-Y)X}^+]}{[\text{Cu(L-Y)}^{2+}] \times [\text{X}^-]} \quad (5)$$

Solutions with millimolar concentrations of Cu(II) complex and ligand concentrations, $0 \leq [\text{X}^-] \leq 10^{-2}$ M, were used for the experiments. Typically, $K_1 \approx 3.6 \times 10^3 \text{ M}^{-1}$ for $\text{Y} = \text{NO}_2$, $\text{X}^- = \text{I}^-$ and $K \approx 5.0 \times 10^2 \text{ M}^{-1}$ for $\text{Y} = \text{NH}_2$, $\text{X}^- = \text{CN}^-$ in methanolic solutions. In agreement with the co-ordination of the anions to the Cu(II) indicated by the spectral changes, the values of K_1 are larger than those expected for the formation of ion-pairs. In the UV region, the changes with the addition of X^- combine the displacement of the absorption bands and the appearance of new absorption bands. Outside the absorption bands of X^- , the spectral difference between $\text{Cu(L-NO}_2\text{)}^{2+}$ and $\text{Cu(L-NO}_2\text{)X}^+$ are associated with a different position of the amino to Cu(II) charge transfer transitions and the contribution of the X^- to Cu(II) charge transfer transitions in the spectrum of $\text{Cu(L-NO}_2\text{)X}^+$. A disruption of the isosbestic points at concentrations of X^- , $[\text{X}^-] \geq 5 \times 10^{-2}$ M, suggested the existence of additional equilibria after the saturation of the Eq. (4). The disruption of the isosbestic points can be attributed to the co-ordination of a second ligand to give Cu(L-Y)X_2 with $K_2 = [\text{Cu(L-Y)X}_2]/([\text{Cu(L-Y)}^{2+}] \times [\text{X}^-]^2) < 10^3 \text{ M}^{-2}$.

3.2. Reduced moieties

The pulse radiolysis technique was used for an investigation of the species produced in the reduction of $\text{Cu(L-NO}_2\text{)}^{2+}$, $\text{Cu(L-NH}_2\text{)}^{2+}$ and Cu(L-H)^{2+} by e_{sol}^- and $\text{CH}_2\text{OH}\bullet$ radicals in aqueous solutions. The reduction of $\text{Cu(L-NO}_2\text{)I}^+$ was investigated with solutions made in CH_3OH . Reactions of the Cu(II) complexes with e_{sol}^- and $\text{CH}_2\text{OH}\bullet$ radicals produced no noticeable absorptions at wavelengths equal to or longer than 400 nm, Fig. 2. A bleach of the bands in the absorption spectrum at wavelengths shorter than 350 nm, i.e., the absorption bands associated with aza to Cu(II) charge transfer optical transitions, were in accordance with the reduction of the Cu(II) species to Cu(I) products.

3.3. Irradiation in CT bands

Deaerated solutions of $\text{Cu(L-NO}_2\text{)X}^+$, $\sim 10^{-4}$ M, in non-aqueous solvents, CH_3CN or CH_3OH , were irradiated at 350 nm with a light intensity, $I_0 \approx 3 \times 10^{-6}$ Einstein $\text{dm}^{-3} \text{ s}^{-1}$. The concentrations of $\text{Cu(L-NO}_2\text{)}^{2+}$ and X^- ,

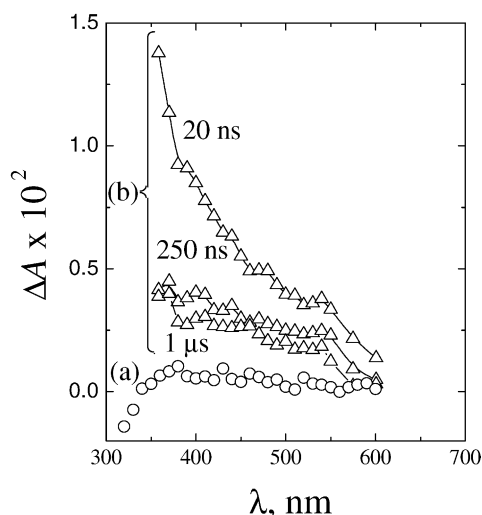


Fig. 2. Transient spectrum: (a), produced in the reduction of $\text{Cu}(\text{L-NH}_2)^{2+}$ with pulse radiolytically generated e_{sol}^- or $\text{CH}_2\text{OH}^\bullet$ radicals. The spectrum (a) is contrasted with the spectrum of I_2^- , (b), produced when $1.5 \times 10^{-3} \text{ M}$ $\text{Cu}(\text{L-NH}_2)\text{I}^+$ in methanolic solutions containing 10^{-2} M I^- was flash irradiated at 351 nm.

$5.0 \times 10^{-3} \leq [\text{X}^-] \leq 2.0 \times 10^{-2} \text{ M}$, were adjusted to insure that $\text{Cu}(\text{L-NO}_2)\text{X}^+$ were the only species absorbing 350 nm light. Solutions of $\text{Cu}(\text{L-NO}_2)^{2+}$, typically 10^{-3} M , were also irradiated at 350 nm. Insignificant changes in the UV–vis spectra of these solutions were observed when they were irradiated a time equal to or less than 4 h. However, colored precipitates were formed with prolonged irradiations, e.g., $t > 24 \text{ h}$. These colored precipitates appear to be more readily formed when $\text{X} = \text{HCO}_2^-, \text{CH}_3\text{CO}_2^-, \text{C}_6\text{H}_5\text{CH}_2\text{CO}_2^-$. Although, the products of the ligand oxidation in the photolysis of $\text{Cu}(\text{L-NO}_2)\text{X}^+$, $\text{X} = \text{halide}, \text{HCO}_2^-, \text{CH}_3\text{CO}_2^-$, could not be successfully isolated, the products of $\text{Cu}(\text{L-NO}_2)(\text{C}_6\text{H}_5\text{CH}_2\text{CO}_2)^+$ were less elusive. Products of the photolysis obtained when the irradiations were limited to periods equal to or shorter than 4 h were analyzed by GC–MS. They revealed that the photolysis products $\text{C}_6\text{H}_5\text{CH}_2\text{OH}$ and $\text{C}_6\text{H}_5\text{CH}_2\text{CH}_2\text{C}_6\text{H}_5$ were in a 10:1 molar relationship. The rapid decarboxylation of the carboxylate radicals produced by the photo-oxidation of or $\text{C}_6\text{H}_5\text{CH}_2\text{CO}_2^-$ must lead to the formation of benzyl radicals, $\text{C}_6\text{H}_5\text{CH}_2^\bullet$. While literature reports indicate that $\text{C}_6\text{H}_5\text{CH}_2\text{CH}_2\text{C}_6\text{H}_5$, is the product of the benzyl radical dimerization [37,38], the relatively large proportion of $\text{C}_6\text{H}_5\text{CH}_2\text{OH}$ suggests that the oxidation of the radicals to form this product is very efficient. When the irradiation of $\text{Cu}(\text{L-NO}_2)(\text{C}_6\text{H}_5\text{CH}_2\text{CO}_2)^+$ was conducted for periods longer than 4 h other products, related to secondary reactions of the benzyl radical, were detected by GC–MS.

Flash photolysis experiments with $\text{Cu}(\text{L-Y})\text{X}^+$ ($\text{Y} = \text{NO}_2$ or NH_2) revealed some of the precursors of the stable products. Transient UV–vis spectra in a $0\text{--}10^2 \mu\text{s}$ time scale were recorded when solutions containing 10^{-4} M $\text{Cu}(\text{L-NH}_2)\text{I}^+$ and $2 \times 10^{-2} \text{ M}$ I^- in CH_3CN or CH_3OH were flash irradiated

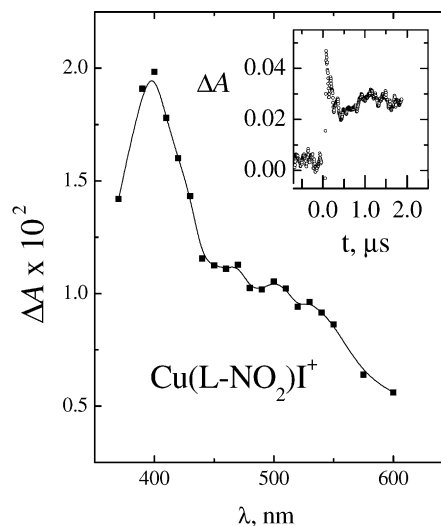
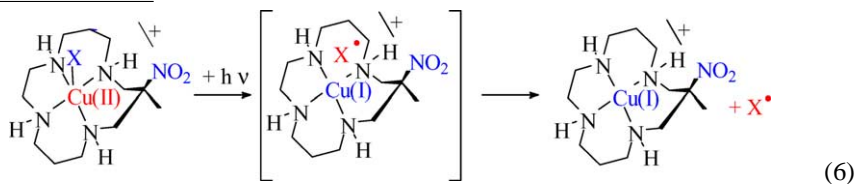


Fig. 3. Transient spectrum recorded $1 \mu\text{s}$ after the 351 nm flash irradiation of $1.5 \times 10^{-3} \text{ M}$ $\text{Cu}(\text{L-NO}_2)\text{I}^+$ in methanol containing 10^{-2} M NaI . Time-resolved changes of 330 nm absorbance are shown in the inset.

ated at 351 nm. Comparisons were made with the spectrum of I_2^- recorded when N_2O -saturated solutions containing $2 \times 10^{-2} \text{ M}$ I^- in CH_3CN or CH_3OH were flash irradiated at 351 nm. The spectra recorded when $\text{Cu}(\text{L-NH}_2)\text{I}^+$ was flash irradiated agreed with the spectrum of the $\text{I}_2^{\bullet-}$ radical, Fig. 2. By contrast, different photoproducts were generated when solutions containing 10^{-4} M $\text{Cu}(\text{L-NO}_2)\text{I}^+$ and $2 \times 10^{-3} \text{ M}$ I^- in CH_3CN or CH_3OH were flash irradiated at 351 nm. The transient spectra differed from the $\text{I}_2^{\bullet-}$ radical spectrum, Fig. 3. Two unstable photoproducts account for the transient spectral changes between 330 and 600 nm. These two species decay with different kinetics. While a shorter lived species absorbs more in the near UV, the longer lived one has a broader spectrum. When the spectrum of the long-lived transient was subtracted from the prompt transient spectrum, i.e., the spectrum recorded immediately after the 20 ns flash, the residual corresponded to the spectrum of $\text{I}_2^{\bullet-}$ radicals.

The formation of the long-lived transient in the photolysis of $\text{Cu}(\text{L-NO}_2)\text{I}^+$ was obscured by the spectrum of $\text{I}_2^{\bullet-}$. In the photolysis $\text{Cu}(\text{L-NO}_2)\text{X}^+$, $\text{X}^- = \text{HCO}_2^-, \text{CH}_3\text{CO}_2^-$, and $\text{C}_6\text{H}_5\text{CH}_2\text{CO}_2^-$, complexes the radicals produced by the oxidation of X^- have spectra with very weak or no absorption bands at wavelengths $\lambda > 400 \text{ nm}$. They provided, therefore, better optical conditions for the observation of the long-lived species. Prompt spectra recorded 10 ns after the irradiation of 10^{-4} M $\text{Cu}(\text{L-NO}_2)\text{X}^+$ in CH_3CN or CH_3OH show maxima at wavelengths, $\lambda_{\text{max}} < 350 \text{ nm}$, Fig. 4. New absorption bands developed in the NIR region during a period of 100 ns, Fig. 4. The growth of these bands is too fast to be ascribed to reactions of the photogenerated radicals with $\text{Cu}(\text{L-NO}_2)\text{X}^+$. The absorption bands in the NIR region grew with axial ligand-dependent rates. For two closely related ligands, $\tau = 34 \text{ ns}$ when $\text{X}^- = \text{C}_6\text{H}_5\text{CH}_2\text{CO}_2^-$ and

$\tau = 46$ ns when $X^- = \text{CH}_3\text{CO}_2^-$. Typical oscillographic traces revealing the growth and the decay of the absorbance in the NIR region are shown in Fig. 4. Curve fitting of the oscillographic traces recorded with $\lambda_{\text{ob}} = 550$ and 625 nm indicated that the decay of the absorbance is kinetically of a second order in the intermediate concentration. In agreement with this rate law, the half lifetime, $t_{1/2}$, exhibited a linear dependence on the reciprocal of the intermediate concentration. A ratio of the rate constant to the extinction coefficient, $k/\epsilon = (1.4 \pm 0.3) \times 10^8 \text{ cm s}^{-1}$ at 560 nm, was calculated from the slope of these linear plots. By contrast to the rate of the absorbance growth, the rate of the absorbance decay was nearly independent of the axial ligand $X^- = \text{HCO}_2^-$,



CH_3CO_2^- , and $\text{C}_6\text{H}_5\text{CH}_2\text{CO}_2^-$. This experimental observation suggests that the same transient species is photogenerated in the photolysis of any $\text{Cu(L-NO}_2\text{)X}^+$ photolyte.

3.4. Irradiation in ligand field bands

Deaerated solutions containing $2.5 \times 10^{-3} \text{ M Cu(L-NO}_2\text{)X}^+$, $X^- = \text{I}^-$, $\text{C}_6\text{H}_5\text{CH}_2\text{CO}_2^-$, and 2.0×10^{-2} to $2.0 \times 10^{-3} \text{ M X}^-$ in MeOH were flash irradiated at 560 nm. Time-resolved spectra recorded in these experiments and those obtained in the 350 nm irradiation of the complexes, Figs. 3 and 4, exhibited similar spectral features and decayed with the same reaction kinetics.

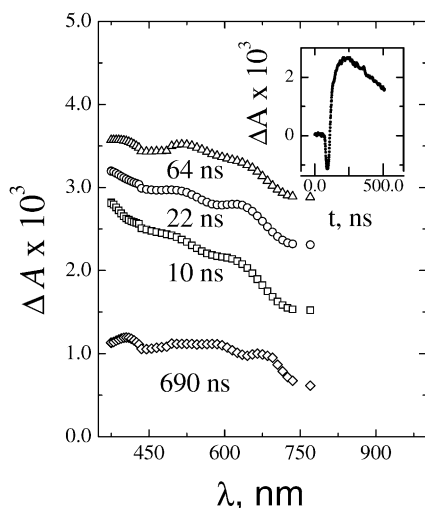


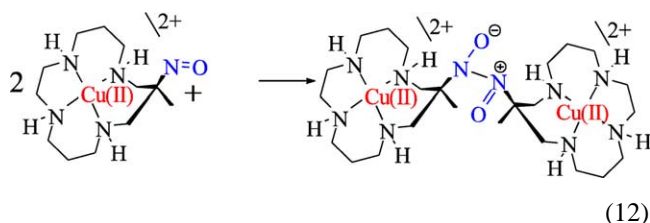
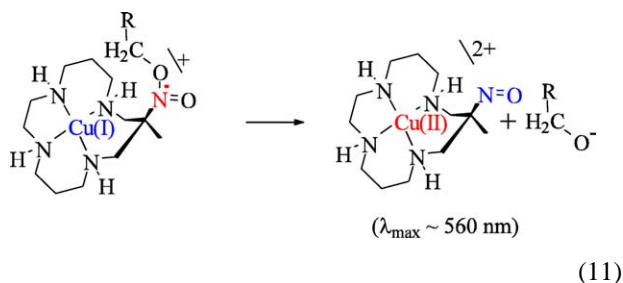
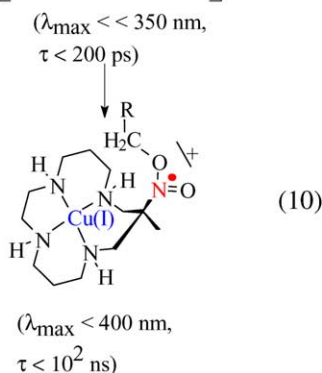
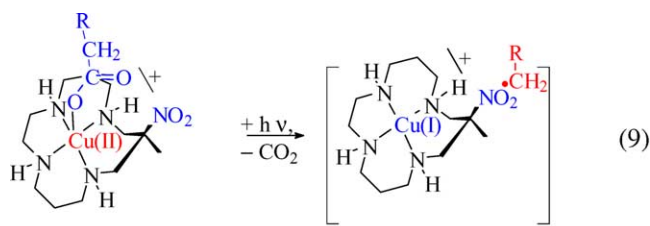
Fig. 4. Difference spectra recorded with various delays after the 351 nm flash irradiation of $3.0 \times 10^{-3} \text{ M Cu(L-NO}_2\text{)C}_6\text{H}_5\text{CH}_2\text{CO}_2^+$ in CH_3CN . A trace for the decay of the flash-generated absorbance is shown in the inset.

4. Discussion

While the photo-oxidation of the axial ligand X^- , appears to be a common process in the ~ 350 nm photochemistry of $\text{Cu(L-NO}_2\text{)X}^+$, $\text{Cu(L-NH}_2\text{)X}^+$ and $\text{Cu(5,7,7,12,14,14-hexamethyl-1,4,8,11-tetraazacyclotetradecane)X}^+$ species, the $-\text{NO}_2$ pendant in $\text{Cu(L-NO}_2\text{)X}^+$ opens new photochemical pathways. In terms of the axial-ligand photo-oxidation, Eq. (6), the products I_2^- and $\text{C}_6\text{H}_5\text{CH}_2\text{CH}_2\text{C}_6\text{H}_5$ in the 350 nm photolyses of $\text{Cu(L-NO}_2\text{)X}^+$ and $\text{Cu(L-NH}_2\text{)X}^+$, $X^- = \text{I}^-$ or $\text{C}_6\text{H}_5\text{CH}_2\text{CO}_2^-$, are accounted for by the characteristic complexation, Eq. (7), and dimerization, Eq. (8), of the radicals X^\bullet ,



Neither the major product of the $\text{Cu(L-NO}_2\text{)C}_6\text{H}_5\text{CH}_2\text{CO}_2^+$ photolysis, i.e., $\text{C}_6\text{H}_5\text{CH}_2\text{OH}$, nor the transients observed in the flash irradiation of $\text{Cu(L-NO}_2\text{)X}^+$ ($X^- = \text{N}_3^-$, HCO_2^- , CH_3CO_2^- , and $\text{C}_6\text{H}_5\text{CH}_2\text{CO}_2^-$) are the unstable species in Eqs. (7) and (8). The longest-lived transient species observed in flash photolysis of $\text{Cu(L-NO}_2\text{)X}^+$ ($X^- = \text{HCO}_2^-$, CH_3CO_2^- and $\text{C}_6\text{H}_5\text{CH}_2\text{CO}_2^-$) have spectra resembling the spectra of nitroso aliphatic compounds [39,40]. They undergo dimerization processes which account for the decay of the transients in a μs – ms time domain via processes that are kinetically of a second order in transient concentration. Moreover, the spectra of the long-lived transients and the values of k/ϵ are independent of the axial ligand X^- suggesting that similar nitroso species, i.e., a species that could be represented as Cu(L-NO)^{2+} , are produced in the photolysis of $\text{Cu(L-NO}_2\text{)X}^+$ ($X^- = \text{I}^-$, HCO_2^- , CH_3CO_2^- , $\text{C}_6\text{H}_5\text{CH}_2\text{CO}_2^-$). A precursor of Cu(L-NO)^{2+} was observed in the 350 nm photolysis of the carboxylate complexes. The presence of this intermediate is revealed in flash photolysis by the prompt spectrum. Because, the prompt spectrum showed some dependence on X^- , it is likely to be a product of the attack by the various X^\bullet radicals on the nitro group. Since, the decarboxylation of CH_3CO_2^- or $\text{C}_6\text{H}_5\text{CH}_2\text{CO}_2^-$ is rapid, the nitro group may trap the C-centered radicals CH_3^\bullet and $\text{C}_6\text{H}_5\text{CH}_2^\bullet$. Adducts similar to those detected in the reactions of CF_3^\bullet radicals with CH_3NO_2 or in the hydrogen abstraction of electronically excited nitro groups will be produced by this attack [41]. On the basis of this precedent, Eqs. (9)–(12) provide a rationale for the sequence of events observed in the flash photolysis of $\text{Cu(L-NO}_2\text{)C}_6\text{H}_5\text{CH}_2\text{CO}_2^+$.



In Eq. (9), the species between brackets denote products of the photolysis in the solvent cage, i.e., transients with a lifetime equal to or less than 10^2 ns. The first product detected in flash photolysis is shown in Eq. (10). Formation of the nitroso product occurs by an intramolecular electronic reorganization, Eq. (11). An alternative process to Eq. (12) is the formation of a binuclear complex, e.g., where the nitroso groups of a partner is coordinated to the metal center of the other. Binuclear nitroso complexes have been isolated [42,43] Although, the formation of the latter species is less probable than the product of Eq. (12), either of them accounts for the experimental observations.

Nitroso products can also be produced when a powerful reductant, i.e., the $\text{CO}_2^{\bullet-}$ radical generated in the photolysis of $\text{Cu}(\text{L}-\text{NO}_2)(\text{HCO}_2)^+$, does not form an adduct with $-\text{NO}_2$. Indeed, a pendant nitro anion radical, $-\text{NO}_2^{\bullet-}$ can be formed by the radical reduction of the pendent $-\text{NO}_2$.

The nitroso product will be subsequently formed when the $-\text{NO}_2^{\bullet-}$ pendent radical is reduced by the Cu(I) center.

The photo-induced reduction of the $\text{Cu}(\text{L}-\text{NO}_2)\text{X}^+$ species can now be contrasted with the redox processes between the complex and the radiolytically generated radicals. In literature reports, the electrochemical reduction of a number of macrocyclic Cu(II) complexes with pendant $-\text{NO}_2$ shows that Cu(II) is reversibly reduced at a potential, $\varepsilon^\circ \approx -0.55$ versus NHE, more positive than the irreversible reduction of the nitro group, $\varepsilon^\circ \approx -0.80$ versus NHE [36]. No $\text{Cu}^{\text{II}}(\text{L}-\text{NO}_2^{\bullet-})\text{X}^+$ species were detected in the pulse radiolytic experiments where $\text{Cu}^{\text{II}}(\text{L}-\text{NO}_2)\text{X}^+$ was reduced with radical. It can be argued that in the radiolytic experiments the radicals produced only a small concentration of $\text{Cu}^{\text{II}}(\text{L}-\text{NO}_2^{\bullet-})\text{X}$ and that this concentration was below the detection limit of the technique. The concentration of $\text{Cu}^{\text{II}}(\text{L}-\text{NO}_2^{\bullet-})\text{X}$ could be kept below the detection limit because the radiolytic radicals reacted slowly with pendant $-\text{NO}_2$ and/or $\text{Cu}^{\text{II}}(\text{L}-\text{NO}_2^{\bullet-})\text{X}$ was rapidly transformed to $\text{Cu}^{\text{I}}(\text{L}-\text{NO}_2)\text{X}$. This mechanism also explains that photo-generated radicals, i.e., the products of Eq. (9), could have escaped the solvent cage and remain undetected in the flash photolysis experiments.

Cu(II) complexes are usually regarded to be photoinert when they are irradiated at wavelengths of the ligand field bands, i.e., they do not induce photochemical reactions whose products can be spectroscopically observed in time scales $t > 10^{-9}$ s. CuCl_2 in poly(vinyl alcohol) film is a known exception to the lack of photochemical activity of the Cu(II) complexes when irradiated in LF bands at $\lambda_{\text{exc}} \geq 680$ nm [44]. The unusual redox photochemistry observed when $\text{Cu}^{\text{II}}(\text{L}-\text{NO}_2)\text{X}^+$ species are irradiated at 560 nm must be rationalized by considering the energy of the X^- to Cu(II) charge transfer transition and the vicinity of reactive $-\text{NO}_2$ groups. Indeed, the redox potentials for the couples $\text{Cu}^{\text{II}}/\text{Cu}^{\text{I}}$

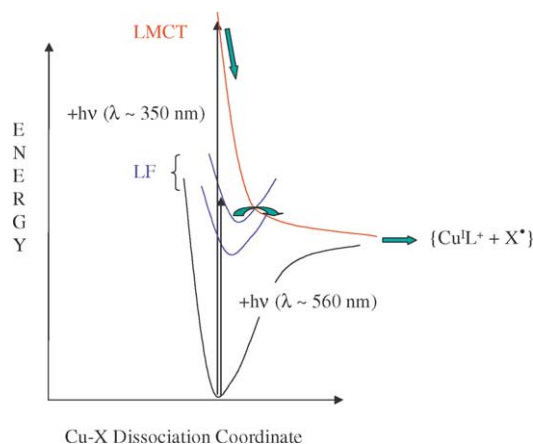


Fig. 5. Electronic states potential energy diagram for the respective irradiations of $\text{Cu}(\text{L}-\text{NO}_2)\text{X}^+$ in ligand-to-metal charge transfer bands, LMCT and $\lambda_{\text{ex}} \approx 351$ nm, and ligand field bands, LF and $\lambda_{\text{ex}} \approx 560$ nm. The product of the geminate photodissociation is represented by $\{\text{Cu}(\text{L}-\text{NO}_2)^+ + \text{X}^-\}$. Transient species observed in flash photolysis are not shown in the figure.

and X^{\bullet}/X^{-} suggest that the threshold for the homolytic dissociation of $Cu^{II}(L-NO_2)X^{+}$ in $Cu^{I}(L-NO_2)^{+}$ and X^{\bullet} fragments, $\sim 150 \text{ kJ mol}^{-1}$, could be very close to the energy of the ligand field excited states placed between 230 and 200 kJ mol^{-1} , Fig. 5. In addition, the efficiency of the geminate photodissociation could be considerably increased because pendent $-NO_2$ groups scavenge the geminate and/or secondary radicals in a time scale shorter than 200 ps. It is therefore possible to use reactive given pendants, attached to a macrocyclic ligand to alter the reaction pathway in addition to change the photophysical processes.

Acknowledgements

This work received support from the Office of Basic Energy Sciences of the U.S. Department of Energy. This is Contribution No. NDRL-4505 from the Notre Dame Radiation Laboratory.

References

- [1] J. Costamagna, G. Ferraudi, B. Matsuhira, M. Campos-Vallete, J. Canales, M. Villagran, J. Vargas, M.J. Aguirre, *Coord. Chem. Rev.* 196 (2000) 125–164.
- [2] A.M. Herrera, G.V. Kalayda, J.S. Disch, J.P. Wikstrom, I.V. Korendovych, R.J. Staples, C.F. Campana, A.Y. Nazarenko, T.E. Haas, E.V. Rybak-Akimova, *Dalton T.* 23 (2003) 4482–4492.
- [3] M. Vicente, R. Bastida, C. Lodeiro, A. Macías, A.J. Parola, L. Valencia, S.E. Spey, *Inorg. Chem.* 42 (2003) 6768–6779.
- [4] R.C. diTargiani, S.C. Chang, M.H. Salter, R.D. Hancock, D.P. Goldberg, *Inorg. Chem.* 42 (2003) 5825–5836.
- [5] S. Aoki, S. Kaido, H. Fujioka, E. Kimura, *Inorg. Chem.* 42 (2003) 1023–1030.
- [6] G. Wei, T.W. Hambley, G.A. Lawrance, M. Maeder, *Aust. J. Chem.* 55 (2002) 667–673.
- [7] E. Kimura, N. Katsube, T. Koike, M. Shiro, S. Aoki, *Supramol. Chem.* 14 (2002) 95–102.
- [8] K.P. Wainwright, *Adv. Inorg. Chem.* 52 (2001) 293–334.
- [9] E. Kimura, S. Aoki, *Biomaterials* 14 (2001) 191–204.
- [10] A.M. Josceanu, P. Moore, S. Smith, *Ann. Chim-Rome* 91 (2001) 517–530.
- [11] E.V. Rybak-Akimova, *Rev. Inorg. Chem.* 21 (2001) 207–298.
- [12] J. Xia, S.A. Li, Y.B. Shi, K. Yu, W. Tang, *J. Chem. Soc. DALTON* (2001) 2109–2115.
- [13] I. Lukes, J. Kotek, P. Vojtišek, P. Hermann, *Coord. Chem. Rev.* 216–217 (2001) 287–312.
- [14] R.R. Fenton, L.F. Lindoy, R.C. Luckay, F.R. Turville, G. Wei, *Aust. J. Chem.* 54 (2001) 59–62.
- [15] P. Comba, S.M. Luther, O. Maas, H. Pritzkow, A. Vielfort, *Inorg. Chem.* 40 (2001) 2335–2345.
- [16] J. Xia, Y. Xu, S.A. Li, W.Y. Sun, K.B. Yu, W.X. Tang, *Inorg. Chem.* 40 (2001) 2394–2401.
- [17] E. Kimura, *Acc. Chem. Res.* 34 (2001) 171–179.
- [18] S. Aoki, H. Kawatani, T. Goto, E. Kimura, M. Shiro, *J. Am. Chem. Soc.* 123 (2001) 1123–1132.
- [19] L. Fabbrizzi, M. Licchelli, P. Pallavicini, A. Perotti, A. Taglietti, D. Sacchi, *Chem. Eur. J.* 2 (1996) 75–82.
- [20] M.E. Padilla-Tosta, J.M. Lloris, R. Martinez-Mañez, A. Benito, J. Soto, T. Pardo, M.A. Miranda, M.D. Marcos, *Eur. J. Inorg. Chem.* 4 (2000) 741–748.
- [21] A.M. Funston, K.P. Ghiggino, M.J. Grannas, W.D. McFadyen, P.A. Tregloan, *Dalton T.* (2003) 3704–3712.
- [22] S. Boyd, N.M. Cabral, K.P. Ghiggino, M.J. Grannas, W.D. McFadyen, P.A. Tregloan, *Aust. J. Chem.* 53 (2000) 651–658.
- [23] G.P. Xue, J.S. Bradshaw, H.C. Song, R.T. Bronson, P.B. Savage, K.E. Krakowiak, R.M. Izatt, L. Prodi, M. Montalti, N. Zaccheroni, *Tetrahedron* 57 (2001) 87–91.
- [24] S. Ronco, G. Ferraudi, in: H.S. Nalwa (Ed.) *Handbook of Photochemistry and Photobiology*, vol. 1, American Scientific Publishers, California, 2003, pp. 316–318 (Chapter 8).
- [25] P.V. Bernhardt, E.G. Moore, M.J. Riley, *Inorg. Chem.* 40 (2001) 5799–5805.
- [26] J. Guerrero, O.E. Piro, M.R. Feliz, G. Ferraudi, S.A. Moya, *Organometallics* 20 (2001) 2842–2853.
- [27] M. Sarakha, G. Ferraudi, *Inorg. Chem.* 38 (1999) 4605–4607.
- [28] G.L. Hug, Y. Wang, C. Schöneich, P.-Y. Jiang, R.W. Fessenden, *Radiat. Phys. Chem.* 54 (1999) 559–566.
- [29] G.V. Buxton, C.L. Greenstock, W.P. Helman, A.B. Ross, *J. Phys. Chem. Ref. Data* 17 (1988) 513–886.
- [30] M.R. Feliz, G. Ferraudi, *Inorg. Chem.* 37 (1998) 2806–2810.
- [31] N. Getoff, A. Ritter, F. Schworer, *Radiat. Phys. Chem.* 41 (1993) 797–801.
- [32] L.M. Dorfman in: R.F. Gould (Ed.) *The Solvated Electron in Organic Liquids*, *Adv. Chem. Series*, vol. 50, Am. Chem. Soc., Washington DC, 1965, pp. 36–44.
- [33] M. Simic, P. Neta, E. Hayon, *J. Phys. Chem.* 73 (1969) 3794–3800.
- [34] G.A. Lawrance, M. O’Leary, *Polyhedron* 6 (1987) 1291–1294.
- [35] G.A. Lawrance, M. O’Leary, B.W. Skelton, F.-H. Woon, A.H. White, *Aust. J. Chem.* 41 (1988) 1533–1544.
- [36] P. Comba, N.F. Curtis, G.A. Lawrance, A.M. Sargeson, B.W. Skelton, A.H. White, *Inorg. Chem.* 25 (1986) 4260–4267.
- [37] H.C. Christensen, K. Sehested, E.J. Hart, *J. Phys. Chem.* 77 (1973) 983–987.
- [38] A.M. Mayouf, H. Lemmetyinen, *J. Photochem. Photobiol. A* 73 (1993) 205–211.
- [39] S. Lacombe, M. Lodett, A. Dargelos, J.M. Canou, *Chem. Phys.* 259 (2000) 1–12, and references therein.
- [40] T.D. Allston, M.L. Fedyk, G.A. Takacs, *Chem. Phys. Lett.* 60 (1978) 97–99.
- [41] J. Lilie, D. Behar, R.J. Sjudak, R.H. Schuler, *J. Phys. Chem.* 76 (1972) 2517–2520.
- [42] E. Colacio, J.M. Dominguez-Vera, A. Escuer, R. Kivekäs, A. Romerosa, *Inorg. Chem.* 33 (1994) 3914–3924, and references therein.
- [43] R.J. Butcher, C.J. O’connor, E. Sinn, *Inorg. Chem.* 18 (1979) 1913–1918.
- [44] N.G. Ignat’ev, A.L. Karasev, V.V. Savel’ev, A.V. Vannikov, *Itz. Akad. Nauk. SSSR, Ser. Khim.* (1986) 676–679.